

Bound $q^2\bar{q}^2$ states in a constituent quark model*

M. W. Beinker[†]

Institut für Theoretische Physik, TU Dresden

B. C. Metsch and H. R. Petry

Institut für Theoretische Kernphysik, Universität Bonn

Abstract

We consider the existence of bound systems consisting of two quarks and two antiquarks ($q^2\bar{q}^2$) within the framework of a constituent quark model. The underlying quark dynamics is described by a linear confinement potential and an effective $q^2\bar{q}^2$ interaction which has its origin in instanton effects of QCD. We calculate the spectra and examine the internal structure of the states found.

I. INTRODUCTION

Most hadrons found experimentally have been identified as mesons ($q\bar{q}$) or baryons (q^3) and their masses and decays can be described fairly well in various quark models. However, there are still a few so-called exotic mesons which can not be interpreted as $q\bar{q}$ states. For the lightest exotic mesons $f_0(975)$ and $a_0(980)$ an underlying $q^2\bar{q}^2$ structure (or $K\bar{K}$ molecule), besides other interpretations (e.g. [1]), has been discussed [2–5], but could not be proved yet unambiguously. Recent experiments and data has renewed the interest in these exotic states [6–9].

We will discuss the existence of bound $q^2\bar{q}^2$ states within a non-relativistic constituent quark model, which was successfully used to describe meson and baryon mass spectra [10] and decays. We can compare the states of this four particle problem with uncorrelated two-meson states and thus obtain a first clue whether the calculated states in reality would be bound or dissociated. In addition, the model is just simple enough to make the calculation of this real four particle problem possible.

We consider the three lightest quark flavours u , d and s , where the constituent quark masses of n and s (n stands for a u or d) are assumed to differ. The potential part of the

*Submitted to Z. Phys. A

[†]E-Mail: beinker@ptprs10.phy.tu-dresden.de

Hamiltonian consists of a sum of two-body forces. This contains a long range, colourdependent confinement part and a short range instanton induced interaction, which is generalized to three flavours [10].

The hamiltonian was calculated in a full basis of solutions of the 3×3 -dimensional harmonic oscillator. Solving the eigenvalue problem and by a variational principle yield the mass spectra and the corresponding eigenstates for further examination of the internal structure of the states.

II. THE MODEL

For calculating the $q^2\bar{q}^2$ states, we used a Hamiltonian of the form

$$H = M + K + V_{\text{conf}} + W \quad (1)$$

where

$$M = \sum_i m_i$$

is the sum of the four constituent quark masses and

$$K = \sum_i \frac{p_i^2}{2m_i} - \frac{P^2}{2M}$$

the kinetic energy for the relative motion.

As confinement potential V_{conf} , we choosed a linear rising potential with the relative quark-(anti)quark distance:

$$V_{\text{conf}}(r_{ij}) = \sum_{i<j} F_C(a_{ij} + b_{ij}r_{ij}).$$

The offset a_{ij} and the slope b_{ij} are different for qq and $q\bar{q}$ confinement. As noted in [11] $a_{q\bar{q}}$ and $b_{q\bar{q}}$ are not independent. The dependence of b_{qq} from $b_{q\bar{q}}$ is given by geometrical reasons [13]. The following relations should hold:

$$\begin{aligned} a_{q\bar{q}} &= -2\sqrt{b_{q\bar{q}}} \\ b_{qq} &= 0.5493^{-1}b_{q\bar{q}} \end{aligned}$$

Although the parameters were independently varied, the above relations in the present approach are fulfilled with great accuracy. They are given in table I. We consider two different kind of colour dependencies F_C of V_{conf} , which in the meson or baryon case are identical. In the first case, F_C is identical to the colour singlett projector P_C^1 [4,5]:

$$V_{\text{conf}}^1(r_{ij}) = \sum_{i<j} P_C^1(a_{ij} + b_{ij}r_{ij})$$

whereas in the other case we have:

$$V_{\text{conf}}^\lambda(r_{ij}) = \sum_{i < j} \frac{\lambda_i}{2} \cdot \frac{\lambda_j}{2} (a_{ij} + b_{ij} r_{ij})$$

with λ_i is a Gell-Man matrix. The V_{conf}^1 potential acts only on colour singletts. In the case of $q^2\bar{q}^2$ only the four $q\bar{q}$ pairs will be affected. Since it is an purely attractive potential two distinct $q\bar{q}$ colour singlett states (which we call quasi-mesons) will always have a net attraction, because also $q\bar{q}$ pairs with q and \bar{q} from different quasi-mesons have always colour singlett contributions yielding unwanted long range forces.

The V_{conf}^λ potential has a better behaviour for $R \rightarrow \infty$, R is the distance of the two quasi-mesons. As was shown [14], it goes with R^{-3} as R grows large which is a consequence of the repulsive part of V_{conf}^λ , which is an effect without experimental evidence. In addition V_{conf}^λ allows a better comparison with earlier results of other authors [4,5].

Finally,

$$W = H_{q_1q_2} + H_{\bar{q}_3\bar{q}_4} + H_{q_1\bar{q}_3} + H_{q_2\bar{q}_4} + H_{q_1\bar{q}_4} + H_{q_2\bar{q}_3}$$

is the residual quark-(anti)quark interaction. The q_1q_2 term is of the form

$$H_{q_1q_2} = -\tilde{g}(P^{S=1}P_6^C + 2P^{S=0}P_3^C)\delta^3(\vec{r})$$

where the flavour matrix \tilde{g} is shown in table II, P^S are spin projectors on the relative qq spin state and P^C denotes a colour projector. \vec{r} is the relative distance of the two quarks. The $\bar{q}\bar{q}$ term is of the same form, if one changes all colour to anticolours and all flavour to their ant flavour indices. All $q\bar{q}$ terms are of the form

$$H_{q\bar{q}} = \hat{g} \left(\frac{3}{2}P^{S=1}P_8^C + P^{S=0} \left(\frac{1}{2}P_8^C + 8P_1^C \right) \right) \delta^3(\vec{r})$$

where the flavour depending \hat{g} is given in table III (for the calculation of this residual interaction from an effective Lagrangian see [10]).

The matrices \tilde{g} and \hat{g} include the total flavour dependence of W . As one can see from table II, \tilde{g} contains a projector on flavour antisymmetric states, while \hat{g} generates a flavour mixing for $T = 0$ states, which allows to describe the η - η' splitting in the meson case, and lowers the energy of the isovector state.

The more complicated structure of W for $q^2\bar{q}^2$ in comparison to the meson or baryon case is a consequence of the fact that there exist two distinct colour singletts for $q^2\bar{q}^2$ and consequently the terms including P_6^C or P_8^C do not vanish. The residual interaction is a pure contact force and as such leads to an unbound Hamiltonian. Therefore, we have chosen to regularize the interaction by replacing the δ distribution by a Gaussian

$$\delta^3(\vec{r}) \rightarrow \frac{1}{\Lambda^3} \frac{1}{\pi^{\frac{3}{2}}} e^{-\frac{r^2}{\Lambda^2}} \delta_{L,0}$$

where Λ can be interpreted as an effective range of the pairing force. We note that a derivation of the 't Hooft force going beyond the one loop approximation which was used, is expected to such a finite range [10].

For the calculation of the $q^2\bar{q}^2$ mass spectra and the eigenstates, we proceed as follows: The matrix elements of the Hamiltonian (1) are calculated within a spin-flavour $SU(6)$, $O(3)$

oscillator basis for each relative coordinate comprising $N = 8$ oscillator excitations in total. We should note that this size of the model space is still too small for reaching convergence of the spectra.

Calculations with $N > 8$ oscillator excitation were limited by the calculational effort. However, the comparison with meson calculations shows that the lowest eigenvalues are calculated with an accuracy of a few MeV.

We obtained the $q^2\bar{q}^2$ spectra by application of the variational principle, i.e. diagonalisation of the Hamiltonian in the oscillator basis and minimization of the lowest energy eigenvalue with respect to the oscillator length parameter. This is consistent to the earlier meson and hadron calculations in [10]. The parameters entering the present calculation are given in table I. These parameter were fitted to the meson and baryon spectra.

III. THE SPECTRA

Fig. 1 shows the mass spectra in the most interesting scalar isoscalar and isovector channel. The columns for each channel are divided into four subcolumns, which show from left to right the sum of the experimental masses of two mesons, the sum of two meson masses calculated with the the same model in the meson sector, the calculated $q^2\bar{q}^2$ spectra with V_{conf}^1 and, finally, the spectra calculated with V_{conf}^λ . In addition, the very left subcolumns shows the masses of $f_0(975)$ and $a_0(980)$, the most popular $q^2\bar{q}^2$ candidates.

The $q^2\bar{q}^2$ eigenvalues are denoted by $n^{2S+1}L^{p_{12}p_{34}}$ where S is the total spin, L the total angular momentum and p_{12} resp. p_{34} the exchange symmetrie of q_1 with q_2 and \bar{q}_3 with \bar{q}_4 respectively. n counts all states with identical S , L , p_{12} and p_{34} .

The two meson-state masses, which are compared with the $q^2\bar{q}^2$ spectra, are chosen to have the same observable quantum numbers as the $q^2\bar{q}^2$ states with the two mesons in a relative s -wave. A main diffulty of our $q^2\bar{q}^2$ model is, that we can not describe two free mesons in a finite model space with a finite number of oscillator excitations. Otherwise, it would be impossible to calculate the Hamiltonian. It is therefore necessary to examine the internal structure of the $q^2\bar{q}^2$ states in detail to differentiate real bound $q^2\bar{q}^2$ states from quasi free two meson states.

As one can see from fig. 1, the $q^2\bar{q}^2$ spectra describe in good approximation the lowest two meson mass sum for the spectra calculated with the V_{conf}^1 potential. The lowest state 0^0S^{--} lies under the $m_\pi + m_\pi$ threshold which is due to the strong long range meson-meson attraction from the V_{conf}^1 potential. Since we consider this long range attraction to be unphysical, this does not imply that 0^0S^{--} is in reality a bound $q^2\bar{q}^2$ state. The eigenstates calculated with the V_{conf}^λ , especially the lowest one, have higher energies due to the repulsive part of this potential.

As a consequence of the discretization of the two meson continuum in our variational approach, both spectra contain more eigenstates in the energy region shown than the sum of the masses of two mesons (with the two mesons in a s -wave) would predict. In other words, the spectra alone do not allow to draw any conclusions wether there exist any “real” $q^2\bar{q}^2$ bound states within this model or not. A closer examination of the internal structure of the calculated eigenstates is therefore necessary.

IV. INTERNAL STRUCTURE

To obtain such a closer view of the interpretation of the internal structure of the calculated $q^2\bar{q}^2$ states, we calculated various probability densities. Let us consider the lowest eigenstate 0^0S^{--} . (Unless stated otherwise we refer to the calculation with the V_{conf}^1 potential.) Fig. 2 shows the densities for the various relative distances with $N_{\text{max}} = 2$ and 8. These densities were calculated by summing over all internal quantum numbers and integrating the $q^2\bar{q}^2$ probability density $\Psi_\alpha^\dagger(\vec{u}_1, \vec{u}_2, \vec{u}_3)\Psi_\alpha(\vec{u}_1, \vec{u}_2, \vec{u}_3)$ over all relative coordinates except the relative distance under investigation, with \vec{u}_i denoting a relative coordinate (e.g. the q - \bar{q} -distance) and α a multiindex for all internal quantum numbers.

The $q\bar{q}$ distribution is calculated as:

$$\rho_{q\bar{q}}(\vec{u}) = \sum_\alpha \int d^3\vec{u}_{q_2, \bar{q}_4} d^3\vec{u}_{q_1 \bar{q}_3, q_2 \bar{q}_4} |\Psi_\alpha(\vec{u}, \vec{u}_{q_2, \bar{q}_4}, \vec{u}_{q_1 \bar{q}_3, q_2 \bar{q}_4})|^2, \quad (2)$$

since all four pairs have the same distribution. It is observed that all densities in fig. 2 are spreading with growing N_{max} . While the q - \bar{q} distance (or inner quasi-meson radius) distribution keeps its form, the $q\bar{q}$ - $q\bar{q}$ (or quasi-meson) distance distribution is mostly spread and its form seems to go over in a uniform distribution with rising N_{max} , only slightly modified by the long range part of the V_{conf}^1 potential, as mentioned above.

For higher excited states the $q\bar{q}$ - $q\bar{q}$ distribution gets more complex and broader while the q - \bar{q} distribution again is mostly localised, and the same conclusions as above can be drawn. Comparison with the distribution of π -meson radius within the same model shows that it has nearly the same form as the q - \bar{q} distribution of the lowest $q^2\bar{q}^2$ state 0^0S^{--} (see fig. 2).

At last, we considered the distribution $\rho(z)$ of a single quark on the z -axis given by:

$$\rho(z) = \sum_\alpha \int d^3\vec{x}_1 d^3\vec{x}_2 d^3\vec{x}_3 d^3\vec{x}_4 |\Psi_\alpha(\vec{x}_1, \vec{x}_2, \vec{x}_3, \vec{x}_4)|^2 \delta\left(\frac{1}{M} \sum_{i=1}^4 m_i \vec{x}_i\right) \delta(\vec{x}_1 - \vec{x}) \quad (3)$$

where \vec{x}_i are the absolute coordinates of the (anti-)quarks. The first δ -function ensures that the center of mass is identical with the center of the coordinate system, and $\delta(\vec{x}_1 - \vec{x})$ cancels the integration over \vec{x}_1 ; \vec{x} is defined by:

$$\vec{x} = \begin{pmatrix} 0 \\ 0 \\ z \end{pmatrix}. \quad (4)$$

Surprisingly, the $\rho(z)$ depends only very weakly on N_{max} , so we can neglect this dependence for a qualitative analysis. The distribution has a quite sharp maximum at $z = 0$ and two significant shoulders at $z = \pm 1\text{fm}$. If we make the assumption, that we have a superposition of two Gaussian-like quasi-meson distributions with their maxima separated by a distance $2a$, we would expect a distribution of the form

$$e^{-(x+a)^2} + e^{-(x-a)^2} = e^{-x^2-a^2} (e^{+2ax} + e^{-2ax}) = ce^{-x^2} \cosh(2ax). \quad (5)$$

So we would expect a Gaussian which is modulated by a cosh-function. Now it is possible to write $\rho(z)$ in the form

$$\rho(z) = \sum_i a_i(z) e^{-\frac{z^2}{b_i^2}} \quad (6)$$

where the width b_i is a flavour dependent constant. The coefficient functions $a_i(z)$ corresponding to the Gaussian expansion (6) are shown in the fig. 3.

It is clear to see, that for $z \rightarrow \pm\infty$ the coefficients which give the important contributions to the sum behave much like cosh functions. This gives evidence that the 0^0S^{--} state in fact describes two free quasi-mesons and is not a bound $q^2\bar{q}^2$ system. Although the contributions of the different flavour components change, this picture is qualitatively still correct if one considers the next higher excited states, also for the V_{conf}^λ . That means, *all* states could be most-likely described as free quasi-mesons.

The little local maximum of the $n^2\bar{n}^2$ coefficient in fig. 3 may indicate that there exist a meson-meson attraction for small distances, which is, however, too weak to lead to a bound system.

V. CONCLUSION

We have extended a model, which is well established in the meson and baryon sector, to $q^2\bar{q}^2$ systems, without any change in the interaction.

The interpretation of the results was not easy, because of the difficulty to distinguish $q^2\bar{q}^2$ from bound states and quasi-free mesons. On the basis of the internal structure, i.e. the density for a single quark and its representation as a sum of Gaussians, we believe, however, to have found a good method to identify possible $q^2\bar{q}^2$ states in spite of the background of quasi-free meson states.

On the basis of results presented in this contribution, the only plausible interpretation is that *all* states we calculated correspond to quasi-free mesons. Especially, we found no hint that there exist very tightly bound states of two quarks and two antiquarks. However, this does not yet rule out, that the $f_0(975)$ and $a_0(980)$ mesons are $K\bar{K}$ molecular states, bound by long range forces, as provided e.g. by meson exchange [6].

REFERENCES

- [1] F.E. Close, Yu.L. Dokshitzer, V.N. Gribov, V.A. Khoze, M.G. Ryskin: Lund preprint, LU TP 93-12, (1993)
- [2] R. L. Jaffe: Phys. Rev. D 15 (1977) 267
- [3] J. Weinstein, N. Isgur: Phys. Rev. D 27, (1983) 588
- [4] J. Weinstein, N. Isgur: Phys. Rev. D 41, (1990) 2236
- [5] M. Oka: Phys. Rev. D 31, (1985) 2274
- [6] G. Janssen, B. C. Pearce, K. Holinde, J. Speth: KFA IKP TH 1994-40, ADP 94-23 T, nucl-th/9411021, (1994)
- [7] A. E. Dorokhov, N. I. Kochelev, Yu. A. Zubov: Z. Phys. C 65, (1995) 667 and references therein
- [8] B. Kerbikov: ITEP 17-95, hep-ph/9503385, (1995)
- [9] S. Wyeck, A. M. Green: Nucl. Phys. A 562, (1993) 446
- [10] W. Blask et al.: Z. Phys. A 337, (1990) 327
- [11] D. Gromes: Z. Phys. C 11, (1981) 147
- [12] A. D. Dolgov, V. I. Zakharov, and L. B. Okun: Sov. J. Nucl. Phys., Vol. 20, (1975) 103
- [13] V. Keiner: Diploma thesis, Bonn, (1993)
- [14] M. B. Gavela et al.: Phys. Lett. B 82, (1991) 431
- [15] G. 't Hooft: Phys. Rev. D 14, (1976) 3432
- [16] M. A. Shifman, A. I. Vainshtein, V. I. Zakharov: Nucl. Phys. B 163, (1983) 46

FIGURES

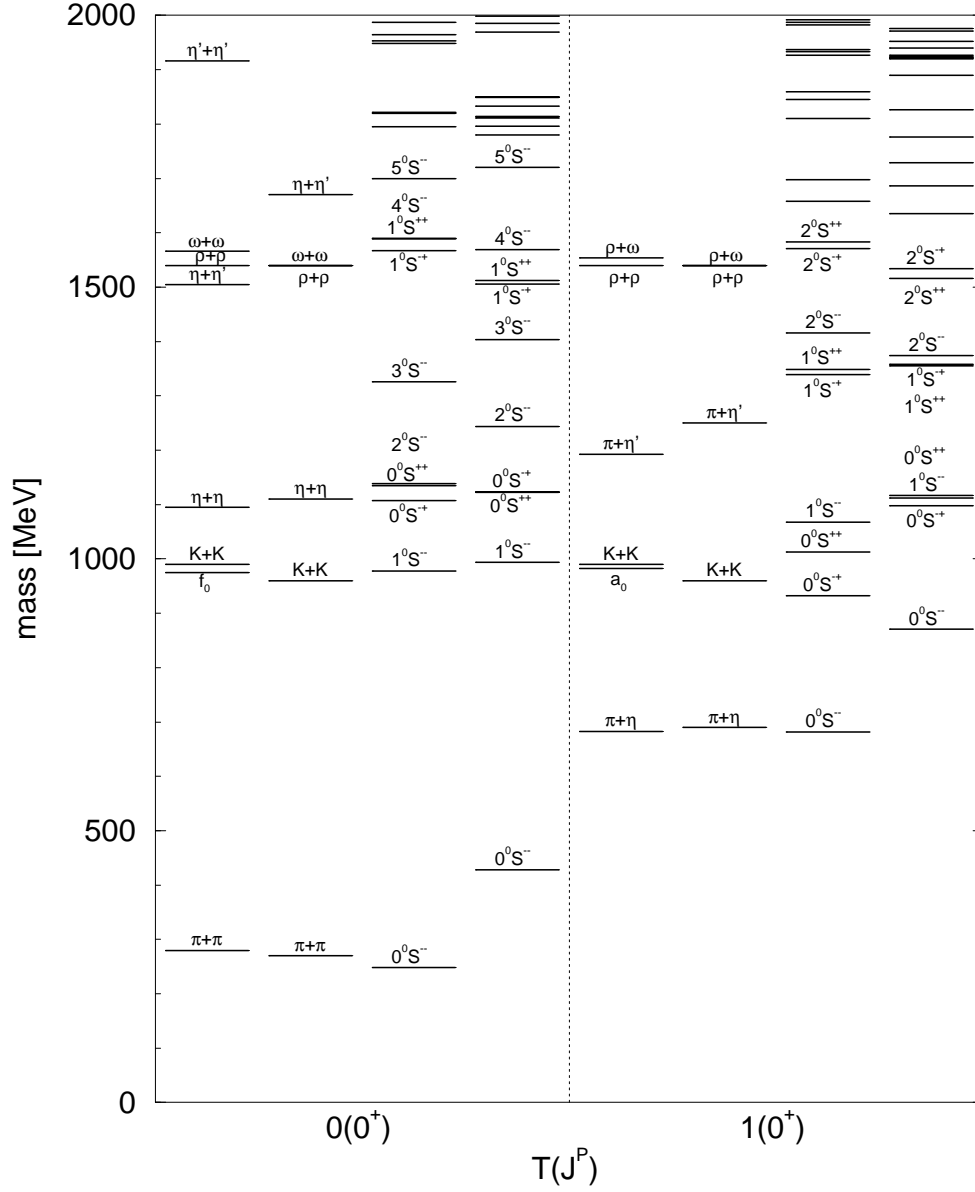


FIG. 1. Spectra for scalar-isoscalar and vector-scalar $q^2\bar{q}^2$ -systems. The subcolumns show from left to right the sum of the experimental masses of two mesons, the sum of two meson masses calculated with the the same model in the single meson sector, the calculated $q^2\bar{q}^2$ spectra with V_{conf}^1 and, finally, the spectra calculated with V_{conf}^λ

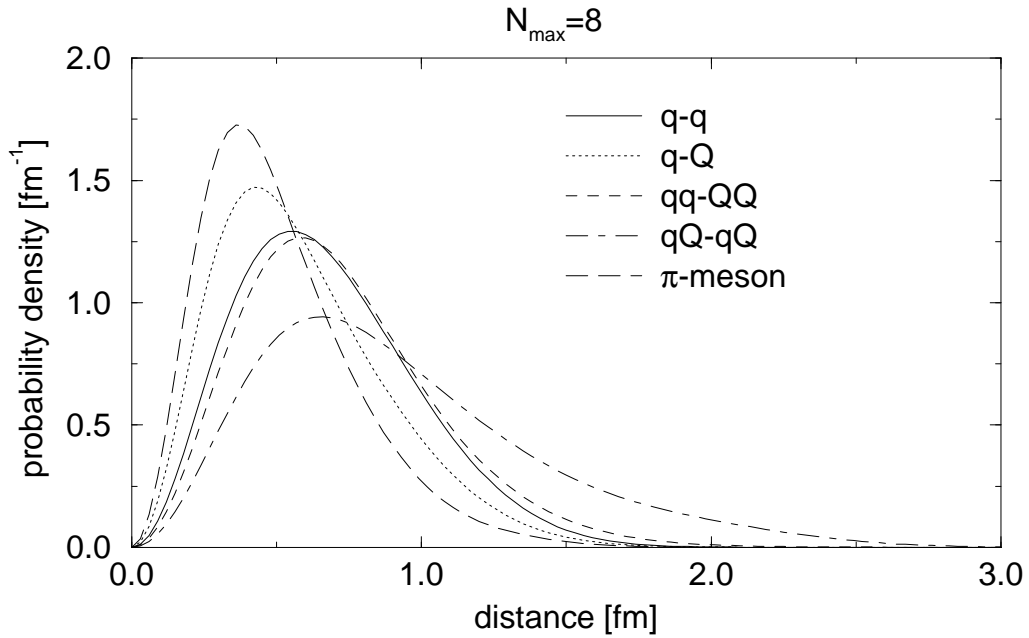
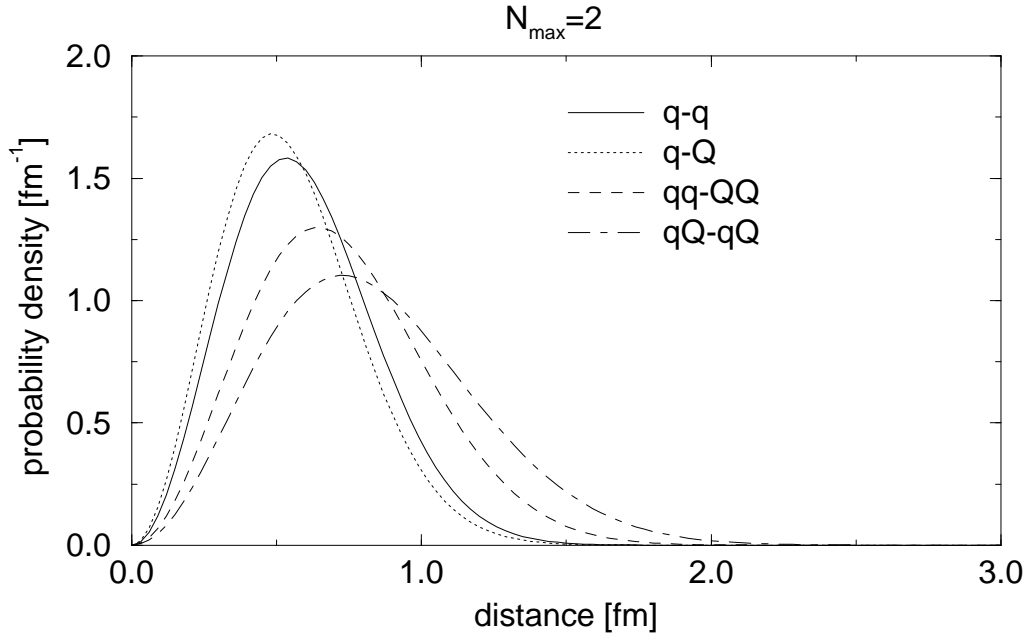


FIG. 2. Density distributions in the channel $0(S^+)$ in dependence of N_{max} . The distributions belong to the ground state. A Q denotes here an anti-quark \bar{q} . For comparison the $q\text{-}\bar{q}$ distribution of the π -meson calculated in the same framework is shown.

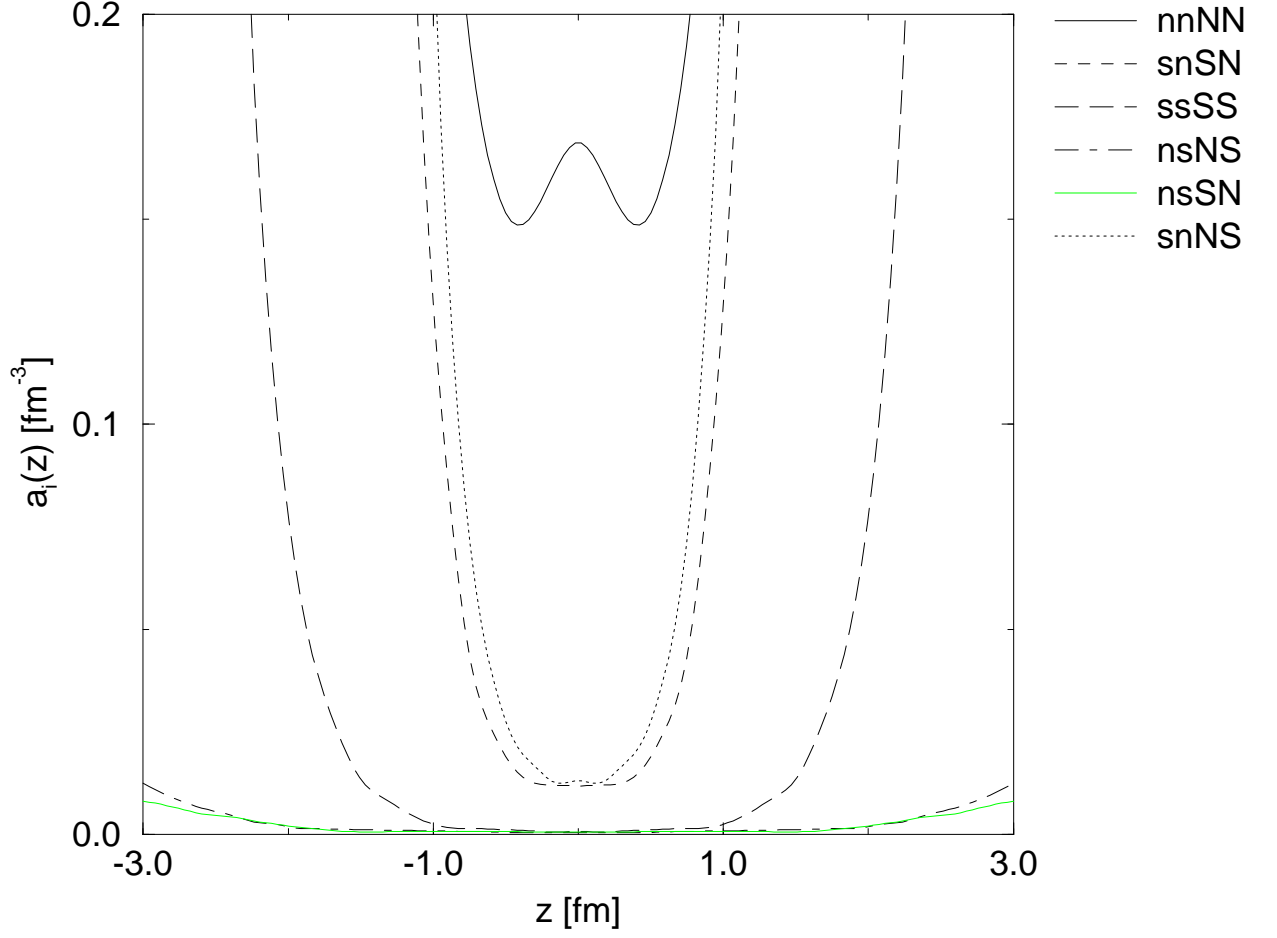


FIG. 3. Coefficient functions belonging to the Gaussian expansion of $\rho(z)$ in (6) for the different flavour components with $N_{max} = 2$. n denotes an u or d quark, a capital letter the corresponding anti-quark.

TABLES

TABLE I. The parameters of the Hamiltonian, fitted to the mass spectra of the light mesons and baryons [10].

m_n	300	Mev
m_s	540	Mev
$a_{q\bar{q}}$	-892	Mev
$b_{q\bar{q}}$	850	Mev fm ⁻¹
a_{qq}	-511	Mev
b_{qq}	467	Mev fm ⁻¹
g	122	Mev fm ³
g'	82	Mev fm ³
Λ	0.37	fm

TABLE II. The flavour matrix \tilde{g} with $g' := \frac{3}{8}g_{\text{eff}}(n)$ and $g := \frac{3}{8}g_{\text{eff}}(s)$.

	ud	du	us	ds	sd	su	uu	dd	ss
ud	g	$-g$							
du	$-g$	g			0			0	
us			g'	0	0	$-g'$			
ds			0	g'	$-g'$	0			0
sd		0	0	$-g'$	g'	0			
su			$-g'$	0	0	g'			
uu									
dd	0				0			0	
ss									

TABLE III. The flavour dependent matrix \hat{g} with g and g' the same as in table II.

	$u\bar{d}$	$d\bar{u}$	$u\bar{s}$	$d\bar{s}$	$s\bar{d}$	$s\bar{u}$	$u\bar{u}$	$d\bar{d}$	$s\bar{s}$
ud	$-g$	0							
$d\bar{u}$	0	$-g$			0			0	
$u\bar{s}$			$-g'$	0	0	0			
$d\bar{s}$			0	$-g'$	0	0			0
$s\bar{d}$		0	0	0	$-g'$	0			
$s\bar{u}$			0	0	0	$-g'$			
$u\bar{u}$							0	g	g'
$d\bar{d}$	0				0		g	0	g'
$s\bar{s}$							g'	g'	0